Intramolecular Hydrogen Bonding and Double H-Atom Transfer in Peroxy and Alkoxy Radicals from Isoprene

Theodore S. Dibble*

Chemistry Department, State University of New York, College of Environmental Science and Forestry, Syracuse, New York 13210

Received: May 29, 2003; In Final Form: December 31, 2003

Quantum mechanical calculations were used to determine the structure and stability of second-generation peroxy and alkoxy radicals formed in the atmospheric degradation of isoprene (2-methyl-1,3-butadiene). Certain of these radicals exhibit a novel hydrogen bonding motif, consisting of two intramolecular hydrogen bonds. The hydrogen bonds are donated in series, with an enol group donating a hydrogen bond to a $-CH_2OH$ group, which donates in turn to the oxygen radical center. This hydrogen bonding motif opens a new reaction pathway: the simultaneous transfer of two H-atoms across the hydrogen bonds with a barrier of only ∼5 kcal/mol in the alkoxy radicals, but ∼20 kcal/mol in the peroxy radicals. Rate constants for these reactions were calculated, and the effects of tunneling on the rate constant were examined. All species and reactions were analyzed at the B3LYP/6-311G(2df,2p) level of theory; the transition states for the double H-atom transfer reactions were also studied using the MPW1K functional and the CBS-QB3 method. Similar chemistry is possible for alkoxy and peroxy radicals derived from other volatile organic compounds of atmospheric interest.

Introduction

Intramolecular and intermolecular hydrogen bonding is well-known to be critical to the structure and function of proteins and nucleic acids in solution. While intermolecular hydrogen bonding is found in the gas phase, including in systems of importance to atmospheric chemistry,[1,2] there are relatively few reports of *intra*molecular hydrogen bonding in gas-phase molecules. This is understandable, since the capacity for intramolecular hydrogen bonding in the gas-phase implies the likelihood of *inter*molecular hydrogen bonds forming in the condensed phase; the natural consequence of intermolecular hydrogen bonds in the condensed phase is a low vapor pressure and minimal importance of the compound in the gas phase. However, computations have revealed intramolecular OH···O hydrogen bonding to be a common motif in β-hydroxyperoxy[3,4] and β-hydroxyalkoxy[3−9] radicals in the atmosphere. These radicals are formed in the gas phase, and react much more rapidly than they can condense. This report describes analogous radicals with not one, but two, intramolecular OH···O hydrogen bonds within a single peroxy or alkoxy radical. Moreover, this structure permits an intramolecular transfer of both H-atoms across the hydrogen bonds, in a single step, at rates which appear to dominate the atmospheric fate of the alkoxy radicals.

Synchronous transfer of two or more protons or H-atoms has been studied in a variety of systems: organic acid dimers;[10] surface or solution phase hydrolysis of atmospheric reservoir species;[11−15] model DNA base pairs;[16,17] and, of course, in solution.[18−20] Hydrogen bond pairs provide a natural mechanism for orienting reactants in ways favorable for synchronous transfer of two hydrogens, so studies of hydrogen bonding go hand in hand with studies of double transfer of H-atoms or protons. This is the case for the double H-atom transfer studied here, because the reactants (and products) may access a variety of hydrogen bonding arrangements.

The peroxy and alkoxy radicals discussed here are formed in the atmospheric degradation of isoprene (2-methyl-1,3-butadiene). The 500 Tg of isoprene emitted to the atmosphere each year, almost exclusively from natural sources, constitutes about 40% by mass of all nonmethane organic compound emissions to the atmosphere.[21,22] Isoprene degradation is initiated primarily by reaction with OH, but only one-half to two-thirds of the mass of the resulting stable products has been specifically identified and quantified.[23] This gap in our knowledge of the atmospheric fate of this important compound motivates our investigations of the chemistry of the peroxy and alkoxy radicals formed in its degradation.

Recent studies[7,9,24−29] have confirmed and refined many aspects of our understanding of isoprene degradation.[30−32] As shown in Figure 1, OH radical adds to the double bond; addition to carbon 1 (∼56%) or carbon 4 (∼37%) produces isoprene−OH adducts[24] (labeled **1** and **4** in Figure 1) which are allylic, and undergo chemically activated (*E*)/(*Z*) isomerization to a significant extent (∼40%).[28] A review of all this chemistry will not be attempted here, rather, the focus is on the reaction pathways leading to the radicals with two intramolecular hydrogen bonds. Subsequent reactions of **1** and **4** lead to formation of the first generation of δ-hydroxyalkoxy radicals **V** and **VI**, in ∼36% and ∼20% yield from **1** and **4**, respectively.[4,30] The (*Z*) isomers of the alkoxy radicals labeled **V** and **VI** are believed to undergo 1,5 H-shift reactions (labeled iso in Figure 1).[28] The allylic radical products can form the dihydroxyperoxy radicals labeled **VII**OO and **IX**OO, and, subsequently, the corresponding alkoxy radicals **VII**O and **IX**O.[28,30]

Although the fractional yield of second generation alkoxy radicals **VII**O and **IX**O are likely rather small (1−2%), their small yields must be put into the context of the enormous isoprene emissions cited above. Their yields are not well-known

* Fax: 315-470-6856. E-mail: tsdibble@syr.edu.

10.1021/jp0306702 CCC: $27.50
Published on Web 03/03/2004

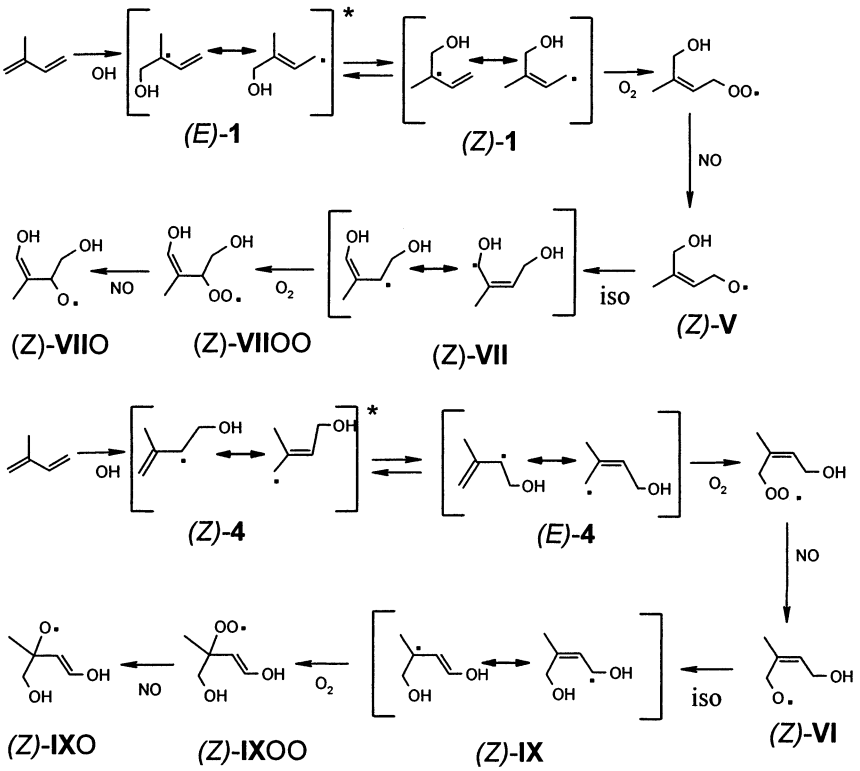

Figure 1. Formation of peroxy radicals **VII**OO and **IX**OO. Several steps have at least one other product, which is omitted for simplicity. The numbering of the radicals is designed to be consistent with that employed by various researchers previously.

because the branching ratios for the formation of the second generation peroxy radicals **VII**OO and **IX**OO from allylic radicals **VII** and **IX** (versus formation of a ketone and HO_2) are unknown.[28] The idea that **VII**O and **IX**O do form is supported by observations of $m/z = 46$ products of their decomposition.[31] The branching ratios for formation of the (*Z*) versus (*E*) isomers of **VII**OO and **IX**OO are not known either.

We attempted to obtain the structures and energies of the transition states for the expected[30] β C−C scission reactions of **VII**O and **IX**O, shown below:

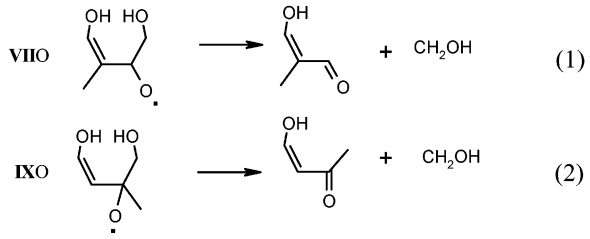

(1)

(2)

Intramolecular OH···O hydrogen bonding to the radical center was expected[3−9] as a structural feature of these alkoxy radicals and their peroxy radical precursors. Analysis of previously published studies of β-hydroxyperoxy and β-hydroxyalkoxy radicals[3,6,33] suggests that the hydrogen bond has little effect on their chemistry or reaction rate constants. So we expected hydrogen bonding but did not expect it to interfere with the rates of reactions 1 and 2. However, the *double* intramolecular hydrogen bonds of the (*Z*) isomers of **VII**O and **IX**O appeared to inhibit the decomposition of these alkoxy radicals. In considering the structural motif of two intramolecular hydrogen bonds, we realized it could also be present in **VII**OO and **IX**OO, the peroxy radical precursors to **VII**O and **IX**O. Moreover, this double hydrogen bonding opens the door to a reaction not previously considered in isoprene chemistry: the simultaneous transfer of two H-atoms across the hydrogen bond.

The remainder of this paper is organized as follows: first, the computational methods are described. The discussion then turns to the structure and energetics of the hydrogen bonding network in peroxy radicals **VII**OO and **IX**OO and the kinetics of their double H-atom transfer reactions. We then consider the hydrogen bonding network of alkoxy radicals **VII**O and **IX**O and the kinetics of their double H-atom transfer reactions. We conclude by analyzing the potential for this chemistry to occur in other radicals of atmospheric interest.

Computational Methods

Quantum chemical computations were carried out using the GAUSSIAN98[34] series of programs. Most calculations used the hybrid exchange functional of Becke[35] and the correlation functional of Lee, Yang, and Parr,[36] a combination denoted B3LYP. Structures and harmonic vibrational frequencies of all species were obtained using B3LYP together with the 6-31G(d,p) basis set. The vibrational frequencies were inspected to verify that transition states possessed only a single imaginary vibrational frequency. The structures of all species were re-optimized at B3LYP/6-311G(2df,2p). All radicals and transition states were treated with the spin-unrestricted formalism. For some transition states, intrinsic reaction coordinate (IRC) calculations were carried out to verify the nature of the transition states, while the identities of other transition states were verified by inspection of their structure and the vector of the imaginary frequency.

The double H-atom transfer represents novel chemistry, and it is desirable to take special care to verify the accuracy of the activation barrier computed for this reaction. Therefore, calculations on the reactants and transition states for the double H-atom transfer reactions were repeated using the Complete Basis Set method CBS-QB3,[37] as well as the MPW1K functional.[38] CBS-QB3 uses a B3LYP structure as the basis of a series of energy calculations to determine relative energies with high reliability.[37]

The MPW1K functional is a modification of the Perdew-Wang functional designed to give improved results for reaction kinetics.[38,39] It has been tested against a set of reactions whose barrier heights are well-known from analysis of experiment.

RRKM-Master Equation calculations were carried out using the UNIMOL program of Gilbert and Smith[40] to obtain thermal rate constants for the double H-atom transfer reactions as a function of pressure at 300 K. Lennard-Jones parameters for the radicals were estimated by the method suggested by Gilbert and Smith[41] to be $\sigma = 6.26$ Å and $\epsilon = 500$ K.

The impact of tunneling on thermal rate constants was estimated by modeling the reaction coordinate with the asymmetric Eckart potential,[42,43] which commonly gives reasonable agreement with more exact computations of tunneling effects.[44] The ratio of the quantum mechanical to the classical rate constant, $\Gamma(T)$, for reactants at a thermal distribution of energy is given by

$$\Gamma(T) = \frac{\exp(V_1/k_B T)}{k_B T} \int_0^\infty \kappa(E) \exp(-E/k_B T)\, dE \qquad (3)$$

where $\kappa(E)$ is the transmission probability. $\kappa(E)$ depends sensitively on the curvature of the barrier, as represented by the imaginary frequency, ν^*, of the vibration along the reaction coordinate. Numerical integration of this expression was carried out using a spreadsheet kindly donated by J. Senosiain.

Results and Discussion

Structural parameters, activation barriers, and energies of reaction reported in the text are derived from B3LYP/6-311G(2df,2p) calculations (with zero-point energies calculated at B3LYP/6-31G(d,p)) unless otherwise specified. Results from all methods are reported in the appropriate tables. The discussion of molecular structure focuses on hydrogen bonding, but a complete set of Cartesian coordinates of key species may be found in the Supporting Information.

A. The Peroxy Radicals. The most stable conformers of the (*Z*) isomers of peroxy radicals **VII**OO and **IX**OO appear to be those in which there are two hydrogen bonds (Figure 2): the enolic hydrogen (on carbon 1 of the isoprene skeleton) donates to the oxygen of the hydroxy group (on carbon 4) adjacent to the radical center, which in turn donates a hydrogen to the radical center. The hydrogen bonds donated from the enol groups are quite short (~1.68 Å), while the hydrogen bonds donated to the radical center are of more usual lengths (1.92−1.95 Å). By contrast, the hydrogen bond to the radical center in $HOCH_2CH_2OO\bullet$, the prototype for intramolecular hydrogen bonds in peroxy radicals, is significantly longer (2.07 Å at B3LYP/6-31G(d,p)).[3,5] From our B3LYP/6-31G(d,p) calculations on **VII**OO and **IX**OO, we know that only a small part (0.02−0.03 Å) of the difference between $HOCH_2CH_2OO\bullet$ and the larger radicals is due to the effect of basis set on the calculated geometry.

VIIOO and **IX**OO can exist in a variety of hydrogen bonding arrangements, which need to be distinguished. At this point, we introduce the nomenclature we use to identify the particular hydrogen bonding arrangements of the radicals. The carbon atoms numbered 1, 3, and 4 in the parent isoprene molecule are bonded to oxygen atoms in **VII**OO. In identifying a hydrogen bond, we use the number of the carbon atom to identify the oxygen atom. An arrow links the number representing the two oxygen atoms participating in a hydrogen bond; the arrow points from the oxygen donating the H-atom to the oxygen atom accepting the hydrogen bond. Therefore, the doubly hydrogen-bonded structure (see Figure 2) is labeled **VII**OO(1→4,4→3). A conformer of the (*Z*) isomer of **VII**OO, lacking the hydrogen bond to the radical center, is therefore denoted **VII**OO(1→4).

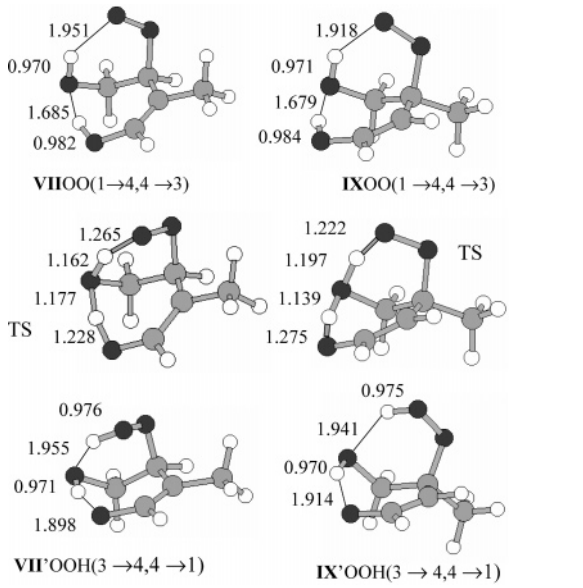

Figure 2. Structures of doubly hydrogen-bonded conformers of second generation peroxy radicals (*Z*)-**VII**OO and (*Z*)-**IX**OO, the transition states (labeled TS) for their synchronous double H-atom transfer, and the products of these reactions. Thin lines indicate hydrogen bonds. O−H distances (B3LYP/6-311G(2df,2p) values, in angstroms) are listed for covalent bonds, hydrogen bonds, and for the breaking/forming bonds in the transition states.

TABLE 1: Relative Energies at 0 K (kcal/mol, including zero-point energies) of Various Conformers of Peroxy Radicals VIIOO, IXOO, and the Products of Their Double H-Atom Transfer

species	B3LYP/ 6-31G(d,p)	B3LYP/ 6-311G(2df,2p)
(*Z*)-**VII**OO(1→4,4→3)	0.0	0.0
(*Z*)-**VII**OO(1→4)	6.3	5.3
(*E*)-**VII**OO(4→3)	5.2	4.1
(*Z*)-**VII′**OOH(3→4,4→1)	−3.7	−3.9
(*Z*)-**IX**OO(1→4,4→3)[a]	−2.0	−2.1
(*E*)-**IX**OO(4→3)[b]	5.6	4.8
(*Z*)-**IX**OO(1→4)[b]	6.8	5.6
(*Z*)-**IX′**OOH(3→4,4→1)[b]	1.7	1.7

[a] Relative to (*Z*)-**VII**OO(1→4,4→3). [b] Relative to (*Z*)-**IX**OO-(1→4,4→3).

For both **IX**OO and **VII**OO, the methyl group is on carbon 2 of isoprene, so a fully consistent numbering scheme for **IX**OO and **VII**OO would yield different numbering patterns for essentially identical patterns of hydrogen bonding. We therefore choose view **IX**OO as an isomer of **VII**OO with the methyl group on carbon 3 rather than carbon 2. Thus, the doubly hydrogen-bonded conformer of **IX**OO is labeled **IX**OO(1→4,4→3).

Conformers of these peroxy radicals possessing only the hydrogen bond from the enolic group, denoted **VII**OO(1→4) and **IX**OO(1→4), are about 5 kcal/mol higher in energy than their doubly hydrogen-bonded counterparts (see Table 1). The (*E*) isomers of **VII**OO and **IX**OO cannot possess a hydrogen bond from the enolic site, and their most stable conformers, (*E*)-**VII**OO(4→3) and (*E*)-**IX**OO(4→3), are about 4−5 kcal/mol higher in energy than their doubly hydrogen-bonded (*Z*) isomers.

TABLE 2: Activation Barriers at 0 K (kcal/mol, including zero-point energies) for Double H-Atom Transfer in Peroxy Radicals VIIOO and IXOO

species	B3LYP/ 6-31G(d,p)	B3LYP/ 6-311G(2df,2p)	MPW1K/ 6-31G(d,p)	MPW1K/ 6-311G(2df,2p)	CBS-QB3
(*Z*)-**VII**OO(1→4,4→3) → (*Z*)-**VII′**OOH(3→4,4→1)	16.3	18.0	24.2	25.7	23.3
(*Z*)-**IX**OO(1→4,4→3) → (*Z*)-**IX′**OOH(3→4,4→1)	19.7	21.5	26.7	28.4	26.8

TABLE 3: Tunneling Corrections (Γ(300K)) for Double H-Atom Transfer in Peroxy Radicals VIIOO and IXOO Computed for Multiple Barrier Heights and Imaginary Frequencies, *ν

species	DFT method for imaginary frequency	*ν** (cm^{-1})[a]	level of theory for barrier height: B3LYP/ 6-311G(2df,2p)	level of theory for barrier height: MPW1K/ 6-311G(2df,2p)	level of theory for barrier height: CBS-QB3
VIIOO	B3LYP	2043	980	6100	3500
	MPW1K	1308	98	12	11
IXOO	B3LYP	2053	3100	15000	11000
	MPW1K	1397	18	22	21

[a] 6-31G(d,p) basis set.

The double hydrogen-bonded structures suggest the possibility of synchronous H-atom transfer reactions 4 and 5:

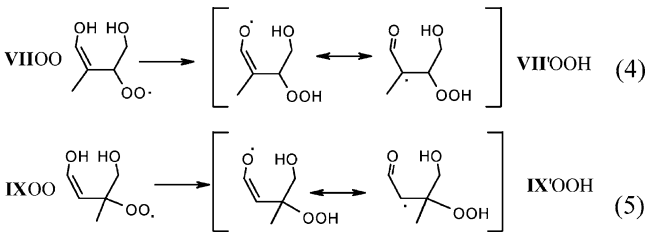

The structures of the transition states (marked TS) and products of these reactions are shown in Figure 2. O−H distances in the transition states are intermediate between the hydrogen bond and covalent bond distances, except that the covalent O−H bond on the β-hydroxy group of the reactant is scarcely lengthened in the transition state. The IRC calculations confirm the nature of the transition state. Because the H-atoms participating in hydrogen bonding in **VII**OO and **IX**OO are in double-well potentials, the products also exhibit double intramolecular hydrogen bonding. The product radicals are labeled **VII′**OOH and **IX′**OOH by analogy to the QOOH notation used for the products of the 1,n H-shift reactions of peroxy radicals in low-temperature combustion.[45,46] The hydrogen bonding arrangements shown in Figure 2 correspond to conformers we denote (*Z*)-**VII′**OOH(3→4,4→1) and (*Z*)-**IX′**OOH(3→4,4→1). These products are alkenoxy radicals, with the two resonance structures indicated in reactions 4 and 5, above. The spin density is about twice as high on the carbon atom as on the oxygen atom.

The potential energy profiles for these reactions are shown in Figure 3 and the relative energies are listed in Tables 1 and 2. The two reactions are roughly thermoneutral. The B3LYP activation barriers of 18.0 and 21.5 kcal/mol imply thermal reaction rate constants (298 K, ignoring tunneling) of ∼0.1 s^{-1} and 4×10^{-4} s^{-1} for **VII**OO and **IX**OO, respectively. Calculations of the rate constant using UNIMOL indicate that these reactions are very nearly at the high-pressure limit at 1 Torr. Using B3LYP values of the imaginary frequency, we calculate that tunneling increases these rate constants enormously, implying rate constants of ∼100 s^{-1} and 1 s^{-1}, respectively (see Table 3). However, the CBS-QB3 and MPW1K barrier heights are ∼5 and ∼7 kcal/mol higher, respectively, than the B3LYP/6-311G(2df,2p) results. Note that at both B3LYP and MPW1K, the barrier heights calculated using the 6-31G(d,p) basis set are 1.5−1.8 kcal/mol lower than those

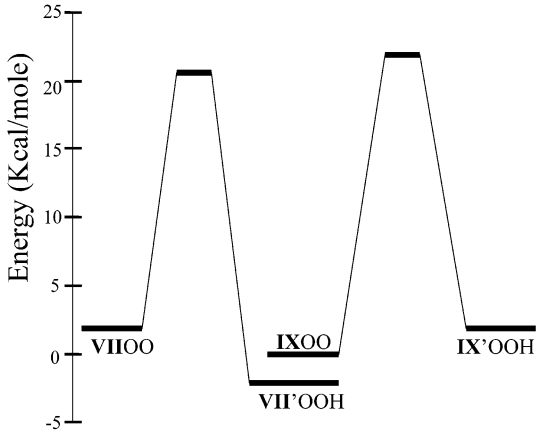

Figure 3. Potential energy profile for double H-atom transfer of peroxy radicals **VII**OO and **IX**OO.

calculated using the 6-311G(2df,2p) basis set.[47] Given the tendency of B3LYP to underestimate barriers to H-atom transfer reactions,[38,39,48] and the good agreement of the CBS-QB3 and MPW1K results, we suspect that the CBS-QB3 and MPW1K results are more accurate. The CBS-QB3 (MPW1K) results imply classical rate constants for **VII**OO and **IX**OO of 1×10^{-5} (2×10^{-7}) s^{-1} and 3×10^{-8} (3×10^{-9}) s^{-1}, respectively, at 298 K. The tunneling corrections to these rate constants (see Table 3) computed using the MPW1K imaginary frequencies to calculate transmission coefficients are only factors of ten to twenty; however, if the B3LYP imaginary frequencies are used, tunneling corrections are about a factor of 10^4. The large uncertainty as to the extent of the tunneling correction deserves more attention and a more exact treatment than the Eckart approach used here. We note that reactions 4 and 5 will not proceed via chemically activated processes, because the barriers to these reactions exceed the expected values of the exothermicity of the reactions which form the peroxy radicals (O_2 addition to allylic radicals).[4]

The dominant fate of **VII**OO and **IX**OO in the polluted atmosphere is reaction with NO, a reaction which possesses a rate constant on the order of $\sim 10^{-11}$ cm^3 $molecule^{-1}$ s^{-1}. Under more pristine conditions, **VII**OO and **IX**OO may react with assorted organic peroxy radicals or with HO_2, at rate constants comparable to that for reaction with NO.[27,33,49] The rate constants discussed above for the double H-atom transfer can be used to determine whether reaction with NO can compete with reactions 4 and 5. Using the CBS-QB3 barrier heights and the higher (B3LYP) tunneling corrections, the concentration of NO needed

to compete with the double H-atom transfer is 3×10^9 molecules cm^{-3} (140 pptv) and 3×10^7 molecules cm^{-3} (1.4 pptv) for **VII**OO and **IX**OO, respectively. Typical NO concentrations are 100 pptv−10 ppbv under polluted conditions, but at least a few pptv even under pristine conditions. This implies that **VII**OO might undergo the double H-atom transfer when [NO] is low but that there is always sufficient NO present to control the fate of **IX**OO.[22,30,33] If one uses the (higher) MPW1K barrier heights and (smaller) tunneling corrections, one would predict that even **VII**OO would not undergo double H-atom transfer under atmospheric conditions. The uncertainty in the activation barriers and tunneling corrections does not permit us to state our conclusions more firmly. At the higher concentrations of NO, HO_2, and organic peroxy radicals commonly used in laboratory experiments, the fate of **VII**OO and **IX**OO will almost certainly be determined by bimolecular reactions.

Reaction of **VII**OO and **IX**OO under polluted condition with NO or NO_3 will form **VII**O and **IX**O in high yield. These reactions are shown below for **VII**OO. Under more pristine

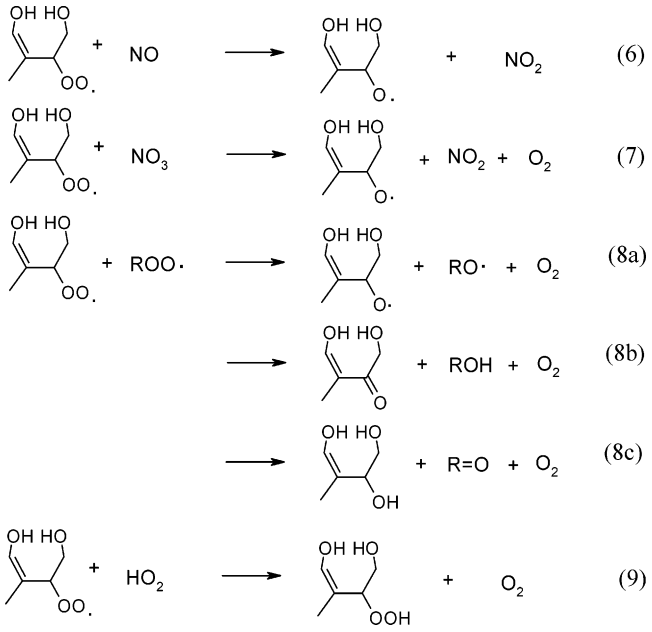

conditions, reaction with various organic peroxy radicals, ROO•, can also produce alkoxy radicals via reaction 8a; however, this occurs in competition with reactions 8b, 8c, and 9, which terminate the organic radical chemistry.

B. The Alkoxy Radicals. The doubly hydrogen-bonded structures of the (*Z*) isomers of **VII**O and **IX**O are the most stable conformers of these alkoxy radicals. Structures of **VII**O and **IX**O are shown in Figure 4, and relative energies are listed in Tables 4 and 5. The hydrogen bond lengths are quite similar to those in the peroxy radicals, namely, those donated from the enolic site are quite short (1.64 Å) while those donated from the β-hydroxy groups are of more normal length (∼2.00 Å). The hydrogen bonds from the β-hydroxy groups are significantly shorter than those in the prototypical β-hydroxyalkoxy radical: $HOCH_2CH_2O$ (2.26−2.27 Å).[3,5]

The nomenclature used here to identify the particular hydrogen bonding arrangements of the **VII**O and **IX**O is exactly analogous to that for **VII**OO and **IX**OO. Figure 5 gives several examples. The **VII**O(1→4) species is 5.8 kcal/mol higher in energy than the doubly hydrogen-bonded conformer **VII**O(1→4,4→3). The hydrogen bond lengths (Figures 4 and 5) and relative energies (listed in Tables 4 and 5 and depicted

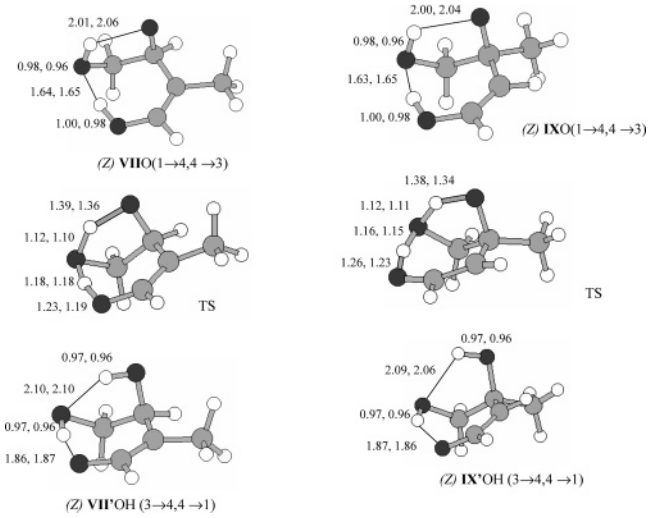

Figure 4. Structures of doubly hydrogen-bonded (most stable) conformers of the (*Z*) configurations of alkoxy radicals **VII**O and **IX**O, the transition states (labeled TS) for their synchronous double H-atom transfer, and the products of these reactions. Thin lines indicate hydrogen bonds. O−H distances (in angstroms) are listed for covalent bonds, hydrogen bonds, and for the breaking/forming bonds in the transition states at B3LYP/6-311G(2df,2p) and MPW1K/6-311G(2df,2p), in that order.

TABLE 4: B3LYP Relative Energies at 0 K (kcal/mol, including zero-point energies) of Conformers and Isomers of VIIO, and the VII′OH Product of the Double H-Atom Transfer

species	B3LYP/ 6-31G(d,p)	B3LYP/ 6-311G(2df,2p)
(*Z*)-**VII**O (1→4,4→3)	0.0	0.0
(*E*)-**VII**O (4→3)	7.5	6.3
(*Z*)-**VII**O (1→4)	6.8	5.8
(*Z*)-**VII**O (4→3)	11.2	9.5
(*Z*)-**VII**O (1→3)	8.2	7.1
(*Z*)-**VII**O (1→3)′	4.6	3.6
(*Z*)-**VII**O (none)	14.0	11.8
(*Z*)-**VII′**OH (3→4,4→1)	−18.6	−19.2

TABLE 5: B3LYP Relative Energies at 0 K (kcal/mol, including zero-point energies) of Conformers and Isomers of IXO, and the IX′OH Product of the Double H-Atom Transfer

species	B3LYP/ 6-31G(d,p)	B3LYP/ 6-311G(2df,2p)
(*Z*)-**IX**O (1→4,4→3)	0.0	0.0
(*E*)-**IX**O (4→3)	7.9	6.9
(*Z*)-**IX**O (1→4)	7.6	6.4
(*Z*)-**IX**O (4→3)	15.0	13.0
(*Z*)-**IX′**OH (3→4,4→1)	−14.8	−15.3

in Figure 6) imply the that the hydrogen bonds donated by the enol groups are strong; the **VII**O(4→3) conformer lies 9.5 kcal/mol above the doubly hydrogen-bonded conformer. The sum of the individual hydrogen bond energies (5.8 + 9.5 = 15.3 kcal/mol) is much greater than their combined energies: 11.8 kcal/mol (Table 4 and Figure 6), implying that formation of the double hydrogen bond creates some strain energy.

The (*E*) isomers of these radicals cannot form intramolecular hydrogen bonds from (or to) the enol groups, and therefore cannot exhibit the double hydrogen bonding motif of the (*Z*) configurations. As a consequence, the (*E*) isomers of these alkoxy radicals are at least 6 kcal/mol higher in energy than in the doubly hydrogen-bonded (*Z*) isomers. The hydrogen bonds to the radical centers are much longer in the (*E*) isomers (2.13−2.15 Å) than in the (*Z*) isomers (∼2.00 Å).

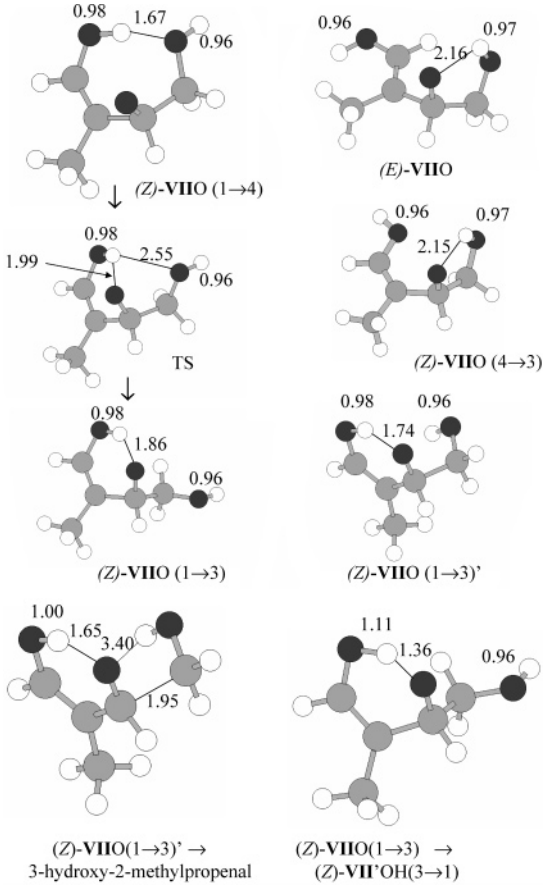

Figure 5. Structures of various conformers of **VII**O with one hydrogen bond, and of the transition state (labeled TS) for rearrangement of hydrogen bonding from alkoxy radical **VII**O(1→4) to **VII**O(1→3). The bottom row depicts structures of transition states for (*Z*)-**VII**O(1→3) decomposing to 3-hydroxy-2-methylpropenal and undergoing single H-atom transfer to form (*Z*)-**VII′**OH(3→1). See text for explanation of the nomenclature describing hydrogen bonding. O−H distances (B3LYP/6-311G(2df,2p) values, in angstroms) are listed for covalent bonds, hydrogen bonds, and for the breaking/forming hydrogen bonds in the transition states.

Let us consider the double H-atom transfer reaction in the (*Z*) isomers of these alkoxy radicals, shown below:

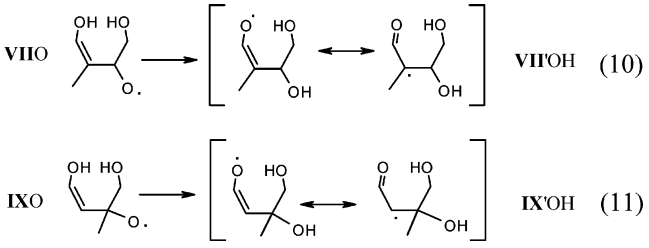

The products are denoted **VII′**OH and **IX′**OH, by analogy with our nomenclature for the products of the double H-atom transfer in the peroxy radicals. Structures for the transition states and reaction products are shown in Figure 4, together with those for the reactants. In the transition state the enolic hydrogen is nearly equidistant from the two oxygens, but the O−H distance of the $-CH_2OH$ group is lengthened by only 0.14 Å from the O−H bond length in the reactant. An IRC calculation confirmed that both H-atoms are transferred together in a single elementary reaction. These reactions are truly H-atom transfers rather than proton transfers; this is clear from the molecular structures shown above and confirmed by the small changes in the Mulliken charges of the oxygen and transferred H-atoms in the course of the reaction. Hydrogen bond lengths in the products are longer than the corresponding lengths in the reactants; this is consistent with the relative weakness of the hydrogen bonds in the products (see below). The MPW1K structures of the transition states are very similar to the B3LYP structures.

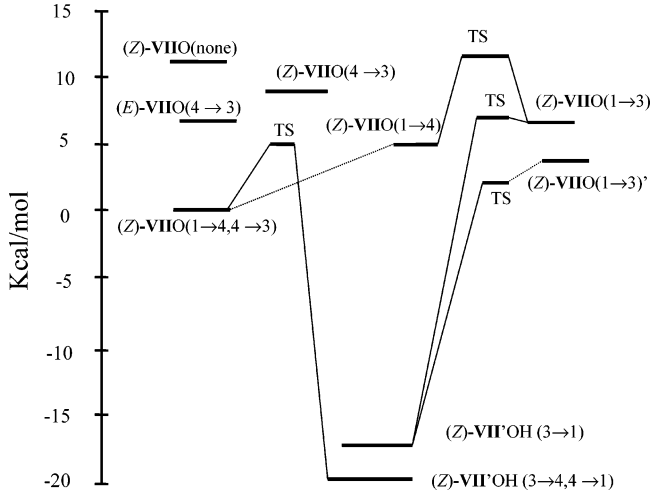

Figure 6. Potential energy profile for hydrogen bonding breaking and rearrangements in (*Z*)-**VII**O.

Unlike the double H-atom transfer in the peroxy radicals, the double H-atom transfer reactions of **VI**O and **IX**O are facile, with barriers of only 4.2 and 4.8 kcal/mol, respectively, at B3LYP/6-311G(2df,2p) (see Table 6). The reaction energies of −19.2 and −15.3 kcal/mol suggest that these reactions are effectively irreversible. These large negative energies of reaction are presumably due to resonance stabilization in the alkenoxy products and the relative instability of alkoxy radicals. It is interesting to note that the computed activation barriers for *reversing* the double hydrogen transfer reactions fall in the narrow range of 20−23 kcal/mol for both alkoxy *and* peroxy radicals. Portions of the B3LYP potential energy profiles for **VII**O and **IX**O are shown in Figures 6 and 7, respectively. CBS-QB3 barrier heights, also listed in Table 6, agree with the B3LYP/6-311G(2df,2p) values to within 0.2 kcal/mol, while MPW1K/6-311G(2df,2p) values are 2.1−2.7 kcal/mol higher than the B3LYP/6-311G(2df,2p) values. Calculations using UNIMOL indicate rate constants of 4×10^8 s^{-1} and 1×10^8 s^{-1}, respectively, at 298 K and 1 atm (3×10^7 s^{-1} and 5×10^6 s^{-1} using the MPW1K activation barriers). The pressure dependence of the classical rate constant at 300 K is shown in Figure 8. The rate constant is clearly in the falloff region at atmospheric pressure. These reactions are much faster than the expected rate of competing *bi*molecular reactions (with NO, NO_2, or, for **VII**O, with O_2).[23, 50]

Tunneling increases the classical rate constant by a factor of 5−16 in the high pressure limit. Here the imaginary frequency is slightly higher at MPW1K (1584 cm^{-1}) than at B3LYP (1387 cm^{-1}). Together with the higher barrier to reaction, the larger curvature at MPW1K causes the computed tunneling correction to be somewhat larger at MPW1K than at B3LYP. This contrasts the case of the peroxy radicals, where the large differences in imaginary frequencies (see Table 3) dominate the tunneling corrections.

The fate of these radicals was expected to be the *uni*molecular β-scission reactions 1 and 2.[30] Experiment and quantum chemical calculations suggest rather low barriers for β-scission

TABLE 6: Activation Barriers at 0 K (kcal/mol, including zero-point energies) for Double H-Atom Transfer in VIIO and IXO

		B3LYP		MPW1K	
reaction	CBS-QB3	6-31G(d,p)	6-311G(2df,2p)	6-31G(d,p)	6-311G(2df,2p)
(*Z*)-**VII**O (1→4→3) → (*Z*)-**VII′**OH (3→4→1)	4.2	2.5	4.0	5.3	6.1
(*Z*)-**IX**O (1→4→3) → (*Z*)-**IX′**OH (3→4→1)	4.6	3.3	4.8	6.7	7.5

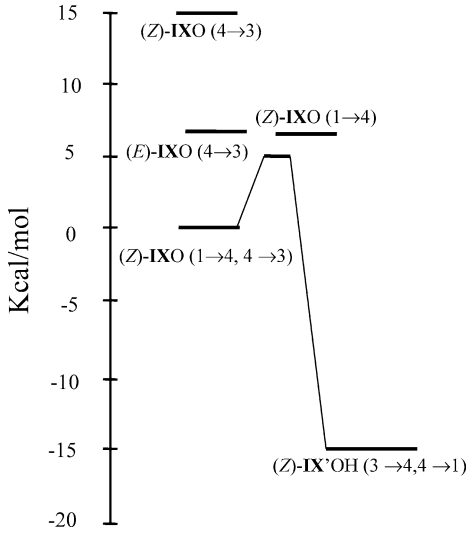

Figure 7. Potential energy profile for hydrogen bonding breaking and double H-atom transfer in **IX**O. Because the conformers of **IX**O were not explored as thoroughly as those of **VII**O, the diagram omits some species and transition states shown in the corresponding plot for **VII**O.

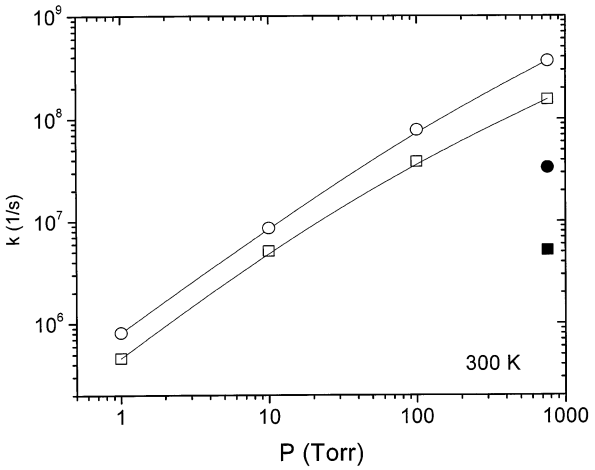

Figure 8. Rate constants for the double H-atom transfer in alkoxy radicals **VII**O (circles) and **IX**O (squares). Pressure dependence at 300 K is calculated using the B3LYP/6-311G(2df,2p) value of the activation barrier (open symbols), while only 760 Torr values were calculated at MPW1K/6-311G(2df,2p) (solid symbols). Lines are merely guides to the eye.

reactions of other β-hydroxyalkoxy radicals,[3,5,6,7,9,50,51] so we searched for transition states for the β-scission reactions, to determine if they could compete with the double H-atom transfer. We were unsuccessful in our attempts to find transition states for the β-scission reactions of the doubly hydrogen-bonded conformers of (*Z*)-**VII**O and (*Z*)-**IX**O. Transition states for β-scission reactions are normally very easy to find,[5,7,9,52] but in (*Z*)-**VII**O(1→4,4→3) and (*Z*)-**IX**O(1→4,4→3) proposed transition state structures were unstable with respect to conformational shifts that broke one or more hydrogen bonds. This instability suggests, though it does not prove, that no transition state exists which directly connects the *doubly* hydrogen-bonded conformers to the products of the β-scission reaction. We do find that β-scission may proceed through conformers with either one hydrogen bond or none. However, in (*Z*)-**VII**O (1→4), which possesses only the stronger hydrogen bond, our attempts to find a transition state for the β-scission of (*Z*)-**VII**O(1→4) obtained, instead, a transition state lying ∼7 kcal/mol above the transition state for the double H-atom transfer (see Table 7). This transition state, which is too high in energy to be important in this chemistry, appears to link (*Z*)-**VII**O(4→3) with the conformer denoted (*Z*)-**VII**O(1→3), but the IRC calculation is ambiguous. Certainly, the energy of this transition state is appropriate to a structure lacking any fully formed hydrogen bonds. Both (*Z*)-**VII**O(1→4) and the transition state which connects it to (*Z*)-**VII**O (1→3), are shown in Figure 5a.

TABLE 7: B3LYP Activation Barriers at 0 K (kcal/mol, including zero-point energies) for Reactions Relevant to VIIO(1→3) and VIIO(1→3)′

reaction	6-31G(d,p)	6-311G(2df,2p)
(*Z*)-**VII**O (1→4) → (*Z*)-**VII**O (1→3)	5.8	5.6
(*Z*)-**VII**O (1→3) → (*Z*)-**VII′**OH (4→3,3→1)	−0.3	0.3
(*Z*)-**VII**O (1→3)′ → (*Z*)-**VII′**OH (4→3,3→1)	−1.8	−1.4
(*Z*)-**VII**O (1→3)′ → Conformer #2 + CH_2OH	5.6	3.5

Conformers lacking the (1→4) hydrogen bond (from the enolic site) are ∼12 kcal/mol higher in energy than the doubly hydrogen-bonded complexes (see Table 4) and will not play a role in the chemistry of (*Z*)-**VII**O and (*Z*)-**IX**O. Therefore, it seems that any transition states for the β-scission reaction of the (*Z*) isomers of **VII**O and **IX**O must lie so much higher in energy than the transition state for the double H-atom transfer as to be unimportant under atmospheric conditions. As noted above, the double H-atom transfer reactions are also much faster than the expected rates of bimolecular reactions of **VII**O and **IX**O. We therefore expect the double H-atom transfer reactions to represent the sole fate of these radicals.

We also investigated another route leading from (*Z*)-**VII**O to (*Z*)-**VII′**OH. The conformer denoted (*Z*)-**VII**O(1→3) is barely stable (0.3 kcal/mol barrier) with respect to a single H-atom transfer leading to (*Z*)-**VII′**OH (3→1). A conformational cousin of (*Z*)-**VII**O(1→3), labeled (*Z*)-**VII**O(1→3)′ is also a potential energy minimum, but the transition state leading from it to (*Z*)-**VII′**OH (3→1) is 2.2 kcal/mol *lower* in energy than reactants after accounting for zero-point energy. (*Z*)-**VII**O(1→3)′ also possesses a low barrier (3.5 kcal/mol) with respect to decomposition. Activation energies of these processes are listed in Table 7.

We attempted to find potential energy minima for (*Z*)-**VII**O(4→3,1→3), that is, a structure with two hydrogen bonds donated to the radical center. The proposed structure of (*Z*)-**VII**O(1→3,4→3) was unstable (not merely metastable) with respect to a single hydrogen transfer from the enol site to form (*Z*)-**VII′**OH(4→3,3→1). This is consistent with the small to negative values of the activation barriers for (*Z*)-**VII**O(1→3) and (*Z*)-**VII**O(1→3)′ transforming to (*Z*)-**VII′**OH(3→1).

The fate of **VII′**OH and **IX′**OH will be determined initially by the competition between prompt decomposition to 3-hydroxy-2-methyl-2-propenal and quenching:

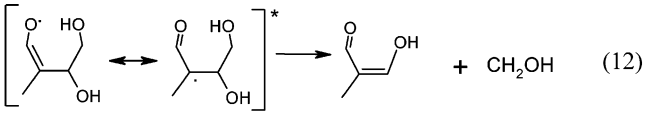

(12)

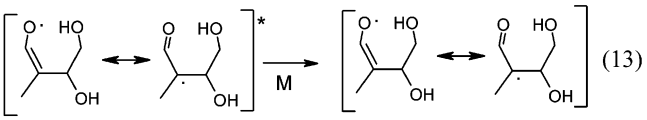

(13)

The study of this competition is the subject of the following paper.[55] Note that the product of reaction 12 is identical to the product of β-scission of **VII**O (reaction 1)! Thermal decomposition of **VII′**OH and **IX′**OH will likely be slow in comparison to addition of O_2 to the carbon possessing radical character.[53] Note that decomposition of **IX′**OH leads to 3-hydroxy-2-butenal:

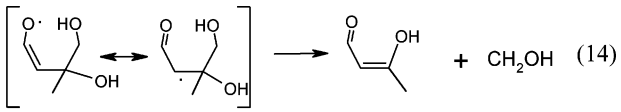

(14)

which is an isomer of the 4-hydroxy-3-buten-2-one product of the decomposition of **IX**O (reaction 2).

C. Generality of the Double H-Atom Transfer in Atmospheric Chemistry. The second generation alkoxy radicals from isoprene may also include the following two species (their source is well-described in refs 28 and 30):

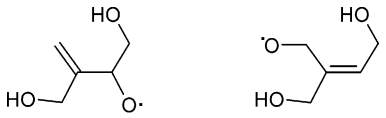

VIIIO **X**O

Intramolecular hydrogen bonding is expected in these radicals, but, unlike in **VII**O and **IX**O, intramolecular hydrogen transfer would not confer the great thermodynamic advantage of resonance stabilization. Therefore, we expect the barriers to intramolecular H-atom transfer to be much higher in **VIII**O and **X**O than in **VII**O and **IX**O, and the fate of **VIII**O and **X**O will likely correspond to the previous predictions: decomposition and reaction with O_2, respectively.[28,30]

The double intramolecular H-atom transfer described herein for radicals derived from isoprene will also occur in radicals derived from 1,3-butadiene (emitted in synthetic rubber production and combustion), because the methyl group of isoprene is just a spectator in the formation of the hydrogen bonds and the subsequent chemistry. As can be seen from Figure 1, the essential elements that lead to this fascinating chemistry are the conjugated double bond of isoprene and a first generation alkoxy radical with sufficient conformational flexibility to undergo the 1,5 H-shift reaction. Certain terpenes, such as myrcene and ocimene, possess conjugated double bonds and may also possess the needed conformational flexibility.[22,54] The first generation alkoxy radicals produced from compounds in which the conjugated double bonds are both part of a ring, as in aromatic compounds and in many other terpenes, are much less likely to undergo 1,5 H-shift reactions, and thus are less likely to create the doubly hydrogen-bonded structures that are necessary for the double H-atom transfer.

Conclusions

Certain conformers of the second generation peroxy and alkoxy radicals expected to be formed in the OH-initiated degradation of isoprene are found to possess two intramolecular hydrogen bonds. These hydrogen bonds are donated in series from an enolic group to a hydroxy group, and from the hydroxy group to the radical center. This structure enables the synchronous intramolecular transfer of two H-atoms, a reaction which is very facile in the alkoxy radicals. However, to the extent the products of the double H-atom transfer undergo prompt or thermal decomposition, there will be little or no atmospheric consequences of this fascinating chemistry.

The synchronous transfer of two H-atoms within a single gas-phase molecule might seem to be a rare event in nature; it is not, at any rate, a commonly studied reaction. However, isoprene is emitted by many species of trees and other vegetation, and so is widely present in a variety of polluted and unpolluted settings; 1,3-butadiene will be widely present in polluted outdoor air. Isoprene also constitutes a significant fraction of the organic compounds emitted in human breath, and may be present in appreciable concentrations inside buildings. Therefore, the necessary ingredients for the intramolecular double H-atom transfer are ubiquitous in air.

Acknowledgment. This research was supported by the National Science Foundation under Grant ATM0087057, and the National Computational Science Alliance under Grant ATM010003N, utilizing the HP-N4000 cluster at the University of Kentucky. The author thanks W. Deng for carrying out the UNIMOL calculations and for assistance with various computing issues, and K. Kitney, L. Zhang, and two anonymous referees for their comments on the manuscript.

Supporting Information Available: Cartesian coordinates of radicals and transition states at B3LYP/6-311G(2df,2p), together with absolute energies of radicals and transition states at all theoretical levels. This material is available free of charge via the Internet at http://pubs.acs.org.

References and Notes

(1) Smith, I. W. M.; Ravishankara, A. R. *J. Phys. Chem. A* **2002**, *106*, 4798.
(2) Aloisio, S.; Francisco, J. S. *Acc. Chem. Res.* **2000**, *33*, 825.
(3) Vereecken, L.; Peeters, J. *J. Phys. Chem A* **1999**, *103*, 1768.
(4) Lei, W.; Zhang, R.; McGivern, W. S.; Derecskei-Kovacs, A.; North, S W. *J. Phys. Chem. A* **2001**, *105*, 471.
(5) Dibble, T. S. *Chem. Phys. Lett.* **1999**, *301*, 297.
(6) Vereecken, L.; Peeters, J.; Orlando, J. J.; Tyndall, G. S.; Ferronato, C. *J. Phys. Chem. A* **1999**, *103*, 4693.
(7) Lei, W.; Zhang, R. *J. Phys. Chem. A* **2001**, *105*, 3808.
(8) Dibble, T. S. *J. Am. Chem. Soc.* **2001**, *123*, 4228.
(9) Dibble, T. S. *J. Phys. Chem. A* **1999**, *103*, 8559.
(10) Miura, S.; Tuckerman, M. E.; Klein, M. L. *J. Chem. Phys.* **1998**, *109*, 5290.
(11) Bianco, R.; Hynes, J. T. *J. Phys. Chem. A* **1998**,*102*, 309.
(12) Hanway, D.; Tao, F.-M. *Chem. Phys. Lett.* **1998**, *285*, 459.
(13) Xu, S. C.; Zhao, X. S. *J. Phys. Chem. A* **1999**, *103*, 2100.
(14) McNamara, J. P.; Tresadern, G.; Hillier, I. H. *J. Phys. Chem. A* **2000**, *104*, 4030.
(15) Loerting, T.; Liedl, K. R. *Chem.-Eur. J.* **2001**, *7*, 1662.
(16) Guallar, V.; Batista, V. S.; Miller, W. H. *J. Chem. Phys.* **1999**, *110*, 9922.
(17) Kawahara, S.; Taira, K.; Uchimaru T. *Chem. Phys.* **2003**, *290*, 79.
(18) Marx, D.; Tuckerman, M. E.; Hutter, J. Parrinello, M. *Nature* **1999**, *397*, 601.
(19) Ando, K. Hynes, J. T. *J. Phys. Chem. **A*** **1997**, *101*, 10464.
(20) Schmitt, U. W.; Voth, G. A. *J. Chem. Phys.* **1999**, *111*, 9361.
(21) Guenther, A.; Hewitt, C. N.; Erickson, D.; Fall, R.; Geron, C.; Graedel, T.; Harley, P.; Klinger, L.; Lerdau, M.; McKay, W. A.; Pierce, T.; Scholes, B.; Steinbrecher, R.; Tallamraju, R.; Taylor, J.; Zimmerman, P. *J. Geophys. Res.* **1995**, *100*, 8873.
(22) Seinfeld, J. H.; Pandis, S. N. *Atmospheric Chemistry and Physics*; Wiley: New York, 1998.
(23) Ruppert, R.; Becker, K. H. *Atmos. Environ.* **2000**, *34*, 1529, and references therein.

(24) McGivern, W. S.; Suh, I.; Clinkenbeard, A. D.; Zhang, R.; North, S. W. *J. Phys. Chem. A* **2000**, *104*, 6609.
(25) Stevens, P. S.; Seymour, E.; Li, Z. *J. Phys. Chem. A* **2000**, *104*, 5989.
(26) Zhang, D.; Zhang, R.; Church, C.; North, S. W. *Chem. Phys. Lett.* **2001**, *343*, 49.
(27) Reitz, J. E.; McGivern, W. S.; Church, M. C.; Wilson, M. D. North, S. W. *Int. J. Chem. Kinet.* **2002**, *34*, 255.
(28) Dibble, T. S. *J. Phys. Chem.* **2002**, *106*, 6643.
(29) Zhao, J.; Zhang, R.; North, S. W. *Chem. Phys. Lett.* **2003**, *369*, 204.
(30) Paulson, S. E.; Seinfeld, J. H. *J. Geophys. Res.* **1992**, *97*, 20703.
(31) Yu, J.; Jeffries, H. E.; Le Lacheur, R. M. *Environ. Sci. Technol.* **1995**, *29*, 1923.
(32) Kwok, E. S. C.; Atkinson, R.; Arey, J. *Environ. Sci. Technol.* **1995**, *29*, 2467.
(33) Jenkin, M. E.; Saunders: S. M.; Pilling, M. J. *Atmos. Environ.* **1997**, *31*, 81.
(34) Frisch, M. J.; Trucks, G. W.; Schlegel, H. B.; Scuseria, G. E.; Robb, M. A.; Cheeseman, J. R.; Zakrzewski, V. G.; Montgomery, J. A. Jr.; Stratmann, R. E.; Burant, J. C.; Dapprich, S.; Millam, J. M.; Daniels, A. D.; Kudin, K. N.; Strain, M. C.; Farkas, O.; Tomasi, J.; Barone, V.; Cossi, M.; Cammi, R.; Mennucci, B.; Pomelli, C.; Adamo, C.; Clifford, S.; Ochterski, J.; Petersson, G. A.; Ayala, P. Y.; Cui, Q.; Morokuma, K.; Malick, D. K.; Rabuck, A. D.; Raghavachari, K.; Foresman, J. B.; Cioslowski, J.; Ortiz, J. V.; Stefanov, B. B.; Liu, G.; Liashenko, A.; Piskorz, P.; Komaromi, I.; Gomperts, R.; Martin, R. L.; Fox, D. J.; Keith, T.; Al-Laham, M. A.; Peng, C. Y.; Nanayakkara, A.; Gonzalez, C.; Challacombe, M.; Gill, P. M. W.; Johnson, B.; Chen, W.; Wong, M. W.; Andres, J. L.; Gonzalez, C.; Head-Gordon, M.; Replogle, E. S.; Pople, J. A. *GAUSSIAN98*, Revision A.6; Gaussian, Inc.: Pittsburgh, PA, 1998.
(35) Becke, A. D. *J. Chem. Phys.* **1993**, *98*, 5648.
(36) Lee, C.; Yang, W.; Parr, R. G. *Phys. Rev. B* **1988**, *37*, 785.
(37) Montgomery, J. A. Jr.; Frisch, M. J.; Ochterski, J. W.; Petersson, G. A. *J. Chem. Phys.* **2000**, *112*, 6532.
(38) Lynch, B. J.; Fast, P. L.; Harris, M.; Truhlar, D. G. *J. Phys. Chem.* **2000**, *104*, 4811.
(39) Lynch, B. J.; Truhlar, D. G. *J. Phys. Chem.* **2001**, *105*, 2936.
(40) Gilbert, R. G.; Smith, S. C.; Jordan, M. J. T. *UNIMOL Program Suite, (*calculation of falloff curves for unimolecular and recombination reactions*)*, 1993. Available from the authors, School of Chemistry, Sydney University, NSW 2006, Australia or by e-mail to gilbert_r@summer.chem.su.oz.au.
(41) Gilbert, R. G.; Smith, S. C. *Theory of Unimolecular and Recombination Reactions*; Blackwell Scientific: Oxford, 1990; p 318.
(42) Eckhart, C. *Phys. Rev.* **1930**, *35*, 1303.
(43) Johnston, H. S. *Gas-Phase Reaction Rate Theory*; Ronald Press: New York, 1966.
(44) Senosiain, J. P.; Musgrave, C. B.; Golden, D. M. *J. Phys. Chem. A* **2001**, *105*, 1669.
(45) Sokolik, A. S. *Self-Ignition, Flame, and Detonation in Gases*; Israel Program for Scientific Translations: Jerusalem, 1963.
(46) Benson, S. W. *Prog. Energy Combust. Sci.* **1981**, *7*, 125.
(47) A referee pointed out that the developers of the MPW1K functional suggested the need of diffuse functions in its use. We carried out calculations at MPW1K/6-311++G(2d, 2p) for the double H-atom transfer in **VII**O, **VII**OO, **IX**O, and **IX**OO. The resulting activation energies were very nearly in the middle of the MPW1K/6-31G(d, p) and MPW1K/6-311G(2df, 2p) results.
(48) Johnson, B. G.; Gonzales, C. A.; Gill, P. M. W.; Pople, J. A. *Chem. Phys. Lett.* **1994**, *221*, 100.
(49) Atkinson, R. *J. Phys. Chem. Ref. Data Monogr.* **1994**, *2*, 28−32.
(50) Atkinson, R. *Int. J. Chem. Kinet.* **1997**, *29*, 99.
(51) Caralp, F.; Forst, W.; Rayez, M.-T. *Phys. Chem. Chem. Phys.* **2003**, *5*, 476.
(52) Ferenac, M. A.; Davis, A. J.; Holloway, A. S.; Dibble, T. S. *J. Phys. Chem. A* **2003**, *107*, 63.
(53) Based on present knowledge of the rate constants for other vinoxy radicals extracted from the NIST Standard Reference Database 17, Version 7.0. $k_{O_2} \sim 1 \times 10^{-12}$ cm^3 molecule^{-1} s^{-1}.
(54) Graedel, T. E. *Rev. Geophys. Space Phys.* **1979**, *17*, 937.
(55) Dibble, T. S. *J. Phys. Chem. A* **2004**, *108*, 2208.